

# Gauge-Fixing Quantum Density Operators At Scale

Amit Jamadagni<sup>1,\*</sup> and Eugene Dumitrescu<sup>1,†</sup>

<sup>1</sup>*Computational Sciences and Engineering Division,  
Oak Ridge National Laboratory, Oak Ridge, Tennessee 37831, USA*

We provide theory, algorithms, and simulations of non-equilibrium quantum systems using a one-dimensional (1D) completely-positive (CP), matrix-product (MP) density-operator ( $\rho$ ) representation. By generalizing the matrix product state’s orthogonality center, to additionally store positive classical mixture correlations, the MP $\rho$  factorization naturally emerges. In this work we analytically and numerically examine the virtual freedoms associated with the representation of quantum density operators. Using this augmented perspective, we simplify algorithms in certain limits to integrate the canonical form’s master equation dynamics. This enables us to quickly evolve under the dynamics of two-body quantum channels without resorting to optimization-based methods. In addition to this technical advance, we also scale-up numerical examples and discuss implications for accurately modeling hardware architectures and predicting their performance. This includes an example of the quantum to classical transition of informationally leaky, i.e., decohering, qubits. In this setting, due to loss from environmental interactions, non-local complex coherence correlations are converted into global incoherent classical statistical mixture correlations. Lastly, the representation of both global and local correlations is discussed. We expect this work to have applications in additional non-equilibrium settings, beyond qubit engineering.

## I. INTRODUCTION

The physical principle of locality refers to the notion that bodies interact (and become entangled) locally in space-time<sup>1</sup>. Locality, in turn, justifies spatio-temporal causality. In addition to its importance for fundamental physics, *information’s* locality holds tremendous implications for efficient computations. Indeed, the cost of transporting data between distant memory locations has become a paradigmatic bottleneck in parallelized and asynchronous post-Moore’s-law computations.

The matrix product state (MPS) rigorously defines the density matrix renormalization group algorithm [1] in terms of a data-structure which maps local data onto a physically localized memory array. Along with new 2D forms [2], these data-structures leverage representation-theoretic redundancies (mathematical gauge invariances) to manifestly encode local properties with local data-structures. In these examples, local properties are locally encoded by gauging multi-linear (ML) tensor network (TN) data structures into canonical forms which satisfy

mathematical constraints [3]. Mapping local properties to local data structures aids in the representation, optimization, and computation of local quantities, even with respect to highly-entangled quantum states. In doing so, ML representations (MLReps) minimize the computational resources in terms of the memory allocation and data communication requirements.

In addition to coherence correlations, responsible for quantum interference phenomena, storing incoherent mixture populations complicates potential scalable representations of density operators ( $\rho$ reps). Prior scalable  $\rho$ rep efforts have been hindered by positivity breaking numerical instabilities—eventually leading to unphysical probabilities—or overly simple models of states and processes which do not accurately capture physically relevant non-equilibrium and open quantum system dynamics. While a rigorous theory has been presented for pure quantum states [3], work is required to elevate density operator ML data-structures to the same level of representation-theoretic mathematical rigor.

In addition to each  $|\psi_k\rangle$ , a density operator

$$\rho = \sum_{k=1}^{\kappa} p_k |\psi_k\rangle\langle\psi_k| \quad (1)$$

contains non-negative ( $0 \leq p_k \leq 1$ )  $L_{1,1}$ -normalized ( $\sum_k p_k = 1$ ) incoherent correlations  $\vec{p} = \{p_1, \dots, p_\kappa\}$ .<sup>2</sup> Given these properties, we call  $\vec{p}$  an *incoherent, classical probability* distribution. In this article we develop machinery to handle and analyze incoherent correlations. In doing so, we see how different physical processes generate

---

This manuscript has been authored by UT-Battelle, LLC, under Contract No. DE-AC0500OR22725 with the U.S. Department of Energy. The United States Government retains and the publisher, by accepting the article for publication, acknowledges that the United States Government retains a non-exclusive, paid-up, irrevocable, worldwide license to publish or reproduce the published form of this manuscript, or allow others to do so, for the United States Government purposes. The Department of Energy will provide public access to these results of federally sponsored research in accordance with the DOE Public Access Plan.

\* [gangapurama@ornl.gov](mailto:gangapurama@ornl.gov)

† [dumitrescu@ornl.gov](mailto:dumitrescu@ornl.gov)

<sup>1</sup> Long ranged interactions originate from *localized* sources and the resulting forces propagate at, or below, the speed of light

<sup>2</sup> Pure states have  $\dim[\vec{p}] = p_1 = 1$ ; thermal states  $\rho_\beta \propto e^{-\beta H}$ , at finite temperature  $T = (\beta k_B)^{-1}$ , have  $\dim[\vec{p}] = \dim[H]$

both local and global incoherent distributions.

In Sec. II, we briefly review amplitudes as coherence correlations, as well as the canonical formulation of the MPS in terms of multi-linear canonical constraints. Sec. III discusses the generalization of the MPS canonical form to one which represents density operators, including both quantum and classical correlations. In Sec. IV, we model processes which convert coherence correlations into mixture correlations. To do so, we entangle qubits and then integrate the open quantum system dynamics to reveal a flow towards noise-localized, informationally-trivial fixed-points. We also examine the dynamics of *global* mixture correlations that emerge from quantum erasure and particle loss channels, with applications to quantum architectures based on photons and atomic traps. Finally, in Sec. V we summarize the key results and further elucidate domains, such as applications to the characterization and engineering of noisy qubits, that can potentially benefit from  $\text{MP}\rho$ 's algorithms.

## II. MATRIX PRODUCT STATES

In this section, we briefly review the notion of coherence correlations as singular values of a quantum wavefunction and show how this leads to the MPS form.

### A. Quantum correlations and entanglement

Consider a pure state  $|\Psi\rangle$  bi-partitioned into left (L) and right (R) regions. The Schmidt decomposition of  $|\Psi\rangle$ , i.e., singular value decomposition (SVD), factorizing the state into L and R degrees of freedom, reads  $|\Psi\rangle = \sum_{\lambda} c_{\lambda} |\psi_{\lambda}\rangle_L \otimes |\phi_{\lambda}\rangle_R$ . Here  $\vec{c} = \{c_1, \dots, c_{\chi}\}$  (see App. A for more details) is a list of quantum *coherence correlation* amplitudes which are  $L_2$ -normalized:  $\sum_{\lambda=1}^{\chi} |c_{\lambda}|^2 = 1$ . When L and R each consist of a single spin-1/2 particle (qubit), the entanglement is maximized by the locus of Bell states which are defined as states with entanglement correlations  $\vec{c} = \{c_1, c_2\} = \{\frac{1}{\sqrt{2}}, \frac{1}{\sqrt{2}}\}$ .

If  $\dim[\vec{c}] = c_1 = 1$ , we have  $|\Psi\rangle = |\psi\rangle_L \otimes |\phi\rangle_R$ , which means that,  $|\phi\rangle$  and  $|\psi\rangle$  are *disentangled* and representable using memory resources describing the *individual* sub-systems. In contrast to the entangled system's multiplicative representational scaling, causing the exponential curse of dimensionality, the memory footprint of disentangled quantum states scales *additively*. A consequence is that the representation and manipulation of disentangled systems is embarrassingly parallelizable.

Tri-partite qubit states may likewise be represented with a correlation vector  $|\Psi\rangle = \sum_{s_i \in \{0,1\}} c_{s_1, s_2, s_3} |s_1\rangle \otimes |s_2\rangle \otimes |s_3\rangle$  where  $s_i$  refers to the region  $i$ 's local Hilbert space. Spin-1/2s (qubits) have  $s_i \in \{\uparrow, \downarrow\}(\{0, 1\})$  while spin-1 particles (qutrits) have  $s_i \in \{\uparrow, 0, \downarrow\}(\{0, 1, 2\})$ , and so on for  $d$ -dimensional systems.

### B. MPS Canonical Form

Instead of *explicitly* storing the coherence correlations, we may *implicitly encode* them via an MLRep. This is indeed the case for the MPS representation [4], where an additional trace over virtual dimensions  $\chi$  encodes coherence correlations as

$$|\Psi\rangle = \sum_{s_i} \text{Tr}_{\chi} [A^{(1)} \cdots A^{(N)}] |s_1\rangle \otimes \cdots \otimes |s_N\rangle, \quad (2)$$

with  $s_i$  now representing the  $i^{\text{th}}$  qubit's computational basis states. The  $A^{(i)}$ 's are multi-dimensional tensors obeying

$$A^{(i)} := A_{\chi_{i+1}}^{\chi_i, s_i} = \mathbb{V}_{\chi_i} \otimes \mathbb{V}_{s_i} \otimes \mathbb{V}_{\chi_{i+1}}^* \rightarrow \mathbb{C}. \quad (3)$$

$\chi$  is called the virtual bond dimension, and it encodes the space of coherent correlations. Equation 2 tells us that the individual amplitudes are found by contracting over the virtual  $\chi$  dimensions associated to the each of the  $A^{(i)}$  tensors. For the remainder of this work we abuse notation and refer to virtual indices by their dimensionality. Following the notation of Ref. 5, the grouping of  $\chi_i, s_i$  as a superscript index and  $\chi_{i+1}$  as a subscript reflects a *left-orthogonalization* with the orthogonality center (OC) at site  $i$ . Similarly, *right-orthogonalization* groups  $s_i$  with  $\chi_{i+1}$  instead of with  $\chi_i$ .

Canonical MPS data-structures are then rigorously defined as those satisfying a pair of quadratic constraints [3]:

$$\sum_i A^{(i)} A^{(i)\dagger} = \mathbb{1}_{\chi_i}, \quad \forall 1 \leq i \neq \text{OC} \leq N, \quad (4a)$$

$$\sum_i A^{(i)} \Lambda^{(i-1)} A^{(i)\dagger} = \Lambda^{(i)}, \quad \forall 1 \leq i \leq N, \quad (4b)$$

where  $\Lambda^{(i)}$  are diagonal, completely (full-rank) positive, and unit trace preserving ( $\text{Tr}[\Lambda^{(i)}] = 1$ ) matrices. The *isometry conditions* of Eq. 4a enable analytic partial trace while Eq. 4b preserves positivity under trace.

The computational complexity of evaluating expectation values, up to a controlled approximation error  $\epsilon$ , using the MPS scales then as  $\mathcal{O}(\text{poly}(N, \chi))$  operations. In the limit  $\chi \ll 2^N$ , where  $N$  is the system size, the computational cost is low in comparison to the state-vector formalism. The opposite limit, of so called *volume-law* states where  $\chi$  is comparable with  $2^N$ , demands high computational resource cost and therefore volume-law systems with higher qubit numbers remain intractable using known classical methods.

## III. $\text{MP}\rho$ : A CLASSICAL/QUANTUM DATA-STRUCTURE

By decorating the MPS data structure, with additional virtual indices, one arrives at the  $\text{MP}\rho$  data-structure.

The decorated degrees of freedom i.e., the new virtual indices, denoted by the  $\kappa$ -index as illustrated in Fig. 1, encode the mixture probabilities. This representation of incoherent mixtures, with a virtual index, is analogous to the role the  $\chi$ -dimensional bonds play in encoding non-local coherent correlations. In the following, we begin by briefly reviewing the concept of mixture correlations. Then, we discuss the holistic integration of coherence and mixture correlations into the  $\text{MP}\rho$  canonical form. Lastly, we present generalized canonical constraints, analogous to the MPS's orthogonality center constraints, in the context of an  $\text{MP}\rho$  canonical form.

We begin by noting a subtle difference between the Matrix Product (Density) Operator, MPO (MPDO) [6, 7] and  $\text{MP}\rho$ . Namely, the virtual  $\kappa$ -mixture indices do not appear in the corresponding MPO(MPDO) representation. As a result, one loses both manifest positivity as well as critical insight into the individual pure components comprising  $\rho$ . In contrast, the locally purified density operator (LPDO)[8] representation does explicitly encode mixture correlations with  $\kappa$ -auxiliary index. As such LPDO is essentially synonymous with  $\text{MP}\rho$ , for a more detailed list of similar representations, see Tab. 1 of Ref. [9]. In order to further emphasize that a local purification is a natural extension of the 1D MPS tensor train, we choose the use of the acronym  $\text{MP}\rho$ . As we will discuss in later sections, invariances amongst the local purification representation may occur when representing global mixture correlations.

A first theme of the current work, is to provide operational constraints for the  $\text{MP}\rho$  and highlight utility in gauging non-unique representations, as is done when defining orthogonality centers in the MPS. As another important point, we discuss how, and when, locally-purified data-structure efficiently encode *global* mixture correlations. Practically, representing global mixture correlations involves selecting a representation which is suitable, in the sense that it minimizes the Kolmogorov-complexity of the representative data structure. One other key result of the current work is to provide a quick algorithm that integrates the two-body channel, within a completely positive  $\text{MP}\rho$  framework without optimization routines. While there have been previous attempts at constructing such an algorithm, these methods rely on optimization routines [8] or consider other memory intensive representations [10] thereby hindering the algorithm's overall scalability.

### A. Classical Mixture correlations

The coherence and incoherent mixture correlations are both *independently* normalized. The coherences are  $L_2$ -normalized,  $\sum_i |c_i|^2 = 1^2$ , while the incoherent mixture correlations are  $L_1$ -normalized,  $\sum_k p_k = 1$ . Note that the SVD is based on the 2-norm, and is therefore a natural fit for optimizing coherence correlations. When using SVD to optimize the  $L_1$  normalized mixtures, an  $L_2$ -

normalized interpretation is that  $\sum_k \sqrt{p_k}^2 = 1^2$ .

To see how both types of correlations co-exist, expand

$$\begin{aligned} \rho &= \sum_k p_k \rho_k = \sum_k p_k |\psi_k\rangle \langle \psi_k| \\ &= \sum_k p_k \left[ \sum_{i=0}^{2^N-1} c_i^{(k)} |i\rangle \right] \otimes \left[ \sum_{j=0}^{2^N-1} c_j^{*(k)} \langle j| \right] \\ &= \sum_{i,j,k} p_k \left[ c_i^{(k)} c_j^{*(k)} |i\rangle \langle j| \right] \end{aligned} \quad (5)$$

where  $c^{(k)}$  are  $|\psi_k\rangle$ 's correlation coefficients and  $\otimes$  denotes *outer* product. Recalling  $\langle n|m\rangle = \delta_{n,m}$ , the trace then unifies both normalizations:

$$\begin{aligned} \text{Tr}[\rho] &= \sum_{l=0}^{2^N-1} \langle l|\rho|l\rangle \\ &= \sum_{k,i,j,l} p_k \left[ c_i^{(k)} c_j^{*(k)} \langle l|i\rangle \langle j|l\rangle \right] \\ &= \sum_k p_k \sum_l |c_l^{(k)}|^2 = \sum_k p_k \times 1 \\ &= 1 \times 1 = 1! \end{aligned} \quad (6)$$

As introduced earlier, the dimension of the virtual  $\kappa$ -index provides insight into the mixture coefficients. That is, at a given site,  $\dim(\vec{p}) = \kappa_i$ . The intuition for  $\text{MP}\rho$  is that the  $k^{\text{th}}$  mixture coefficient  $p_k$  is, via the  $\kappa_i$  index, encoded as the probability for the positive operator  $\vec{A}_k \vec{A}_k^\dagger$ .

Note that the  $\text{MP}\rho$  formalism provides many possible non-unique gauge choices for factorizing the incoherent mixture correlations. For example, in the *local* mixture limit, we can absorb the *global*  $\vec{p}$  probabilities into single tensor i.e., by setting  $p_k^{\frac{1}{2}} A_j^{(k)} = \tilde{A}_j^{(k)}$  for a single  $j$ . Alternatively, global mixtures could be symmetrically decomposed into all local  $c_i$ , simply by setting  $p_k^{\frac{1}{2^N}} A^{(j)} \rightarrow \tilde{A}_k^{(j)}$  for all  $j$ . Independent of the gauge one chooses to store correlations, a further non-uniqueness, characteristic of  $\text{MP}\rho$ , is proven by the illustration in the bottom panel of Fig. 6.

In the rest of this section, we first examine the canonical form and then provide illustrative examples that allow us to gain intuition regarding the functionality of the virtual  $\kappa$  index, as well as factorize classical and quantum correlations together. In doing so, we will provide examples in the opposite limits of local (see Sec. IV A) and global (see Sec. IV C) classical mixture correlations.

### B. $\text{MP}\rho$ canonical form

The  $\text{MP}\rho$ 's non-negative mixture correlations are encoded within a completely positive matrix product operator (CPMPO) [8] representation. The key desirable feature of such a CPMPO is that it *manifestly enforces*

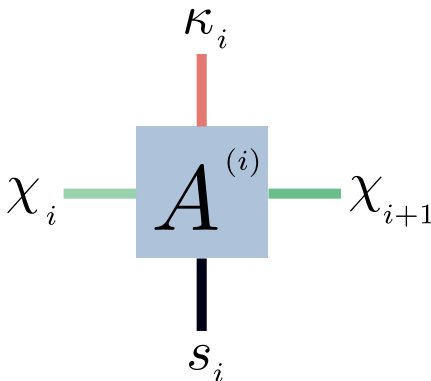


Figure 1. Generalization of the MPS tensor to that of the MP $\rho$  canonical form. We decorate each tensor,  $A^i$ , equipped with a physical index,  $s_i$  and virtual indices  $\chi_i$  and  $\chi_{i+1}$  with an additional index  $\kappa_i$ .

*positivity* via an explicit positive representation  $\rho = \vec{A}^\dagger \vec{A}$ , where  $\vec{A} = \{A_1, \dots, A_N\}$  denotes the tensor train. As illustrated in Fig. 1, the CPMPO's  $A^{(i)}$  tensors are equipped with virtual  $\chi$ -dimensional coherence vector spaces, physical vector spaces  $s_i$ , and now additionally with  $\kappa_i$ -dimensional mixture spaces. This generalizes our prior definition for each site's tensor to

$$A^{(i)} := A_{\chi_{i+1}}^{\chi_i, s_i, \kappa_i} = \mathbb{V}_{\chi_i} \otimes \mathbb{V}_{s_i} \otimes \mathbb{V}_{\kappa_i} \otimes \mathbb{V}_{\chi_{i+1}}^* \rightarrow \mathbb{C}. \quad (7)$$

Note that grouping  $\chi_i$  and  $\kappa_i$  with  $s_i$  foreshadows a left-orthogonality decomposition. Indeed, grouping the top indices together preconditions the tensor for a top  $\times$  bottom-dimensional matrix singular value decomposition. In the limit of  $\kappa_i = 1, \forall i$ , one recovers the MPS data structure. Since it is not always clear how to factorize the mixture correlations, amongst the collection of individual tensors, the dimensionality of each tensors  $\kappa$ -index represents a powerful, latent gauge freedom that we investigate below.

### C. Canonical Constraints

The SVD of the tensor at the  $i^{\text{th}}$  site reads

$$A^{(i)} := A_{\chi_{i+1}}^{\chi_i, \kappa_i, s_i} = U_{\sigma}^{\chi_i, \kappa_i, s_i} \Sigma_{\sigma}^{\chi_i} (V_{\chi_{i+1}}^{\sigma})^T \quad (8)$$

where  $\sigma = \dim(\Sigma) = \min(\dim(U), \dim(V^T))$ . The indexing of the terms in Eq. 8 highlights a right orthogonalization, where the norm is absorbed into the neighboring tensor to the right ( $i+1$ ). After this step, the updated tensors (denoted by overhead tilde) are given by

$$\begin{aligned} U_{\sigma}^{\chi_i, \kappa_i, s_i} &\rightarrow \tilde{A}^{(i)} \\ \sum_{\sigma, \chi_{i+1}} \Sigma_{\sigma}^{\chi_i} (V_{\chi_{i+1}}^{\sigma})^T A_{\chi_{i+2}}^{\chi_{i+1}, \kappa_{i+1}, s_{i+1}} &\rightarrow \tilde{A}^{(i+1)} \end{aligned} \quad (9)$$

where  $\sigma$  is then re-labeled as the new  $\chi_{i+1}$ .

Having factorized a site tensor and subsequently ab-

sorbed the singular value core  $\Sigma$  into the adjacent site, the updated tensor at site  $i$  now obeys the canonical isometric condition. From the perspective of this first tensor, tracing out the first lattice site's physical ( $s_i$ ), and mixture ( $\kappa_i$ ), and left ( $\chi_i$ ) degrees of freedom with its dual yields

$$\text{Tr}[A^{(i)} A^{(i)\dagger}] := \sum_{\chi_i, \kappa_i, s_i} A_{\chi_{i+1}}^{\chi_i, \kappa_i, s_i} (A_{\chi_{i+1}}^{\chi_i, \kappa_i, s_i})^\dagger = \mathbb{1}_{\chi_{i+1}} \quad (10)$$

which is the isometric generalization of Eq. 4a. Like in the MPS case, given a judicious series of matrix decompositions and contractions absorbing the state's norm onto a single orthogonality core tensor, we can fulfill Eq. 10 on all sites to the left and right of an OC.

## IV. NUMERICAL RESULTS

In this section, we present a series of illustrative simulations that provide insight into the inner workings of MP $\rho$ . To do so, we utilize 1- and 2-local Markovian quantum channels to transform entangled resource states into incoherent mixed states of varying locality. Afterwards, we validate the optimization-free two-body quantum channel algorithm by studying the action on analytically solvable Greenberger–Horne–Zeilinger (GHZ) state dynamics. Finally, we examine the form of global mixture correlations that arise due to tracing out a physical degree of freedom, as in a quantum erasure channel.

### A. Local MP $\rho$ attractors

To benchmark quantum computers, one may be interested in quantifying how 1-local dissipative maps destroy quantum coherence correlations, especially at scale. To examine this, we first prepare random MPS states which are characterized by different bond dimensions but defined on an identical  $L$ -site lattice. Note that the product of the spatial extent with bond dimension quantifies the system's total entanglement. Next, we evolve under the action of 1-local noise channels. The noise operators act on the state at each time step, thus defining an open-quantum system clock cycle.

Explicitly, the quantum channel which is applied at each error clock cycle factorizes as the composition of two quantum maps. The first map is a single qubit phase ( $p$ ) damping channel with Kraus operators  $K_0^p = \sqrt{\alpha} \mathbb{1}$  and  $K_1^p = \sqrt{1-\alpha} Z_i$ , where  $Z_i$  is the Pauli- $Z$  acting on site  $i$ , with  $\alpha$  being the dephasing rate. The second channel, the bit-flip ( $b$ ) map, is characterized by the Kraus operators  $K_0^b = \sqrt{\beta} \mathbb{1}$  and  $K_1^b = \sqrt{1-\beta} X_i$  with  $X_i$  being the Pauli- $X$  acting on site  $i$  and  $\beta$  the bit-flip rate.

Intuitively, for any almost-depolarized quantum state in the long time limit, we expect the action of the noise channels to drive the state towards a final form  $\rho_F = (1-\epsilon)\mathbb{1}/D + \epsilon\sigma$  where  $\sigma$  is a non-local remnant of



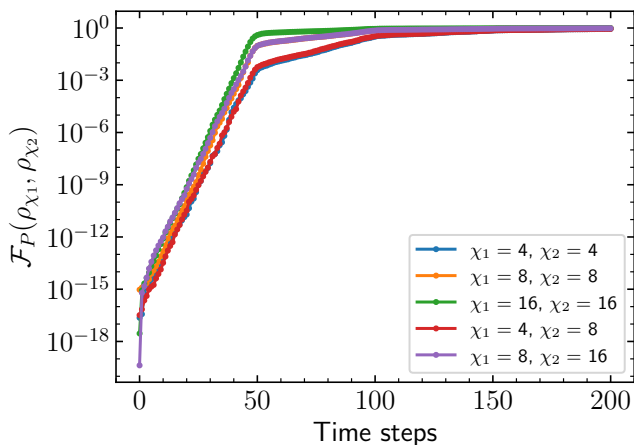


Figure 2. The flow of state fidelities as a function of time steps (clock-cycles) in the presence of 1-body bit and phase flip quantum noise channels. At  $t = 0$ , the randomly initialized states have overlap fidelities  $F_{ij} = \|\langle \psi_i | \psi_j \rangle\|^2 \leq 1E^{-14}$ . By the end of the quantum channel the initially approximately-orthonormal states now have  $1E^{-1} \leq F_{ij} \leq 1$ . The fidelity is computed at each time step with respect to a pair of distinct random states characterized by the bond dimension  $\chi_i$  and  $\chi_j$  respectively, with the system size set to  $N = 50$ . The total number of time steps is given by the number of cycles,  $n_c$ , times the number of sites. Each cycle has  $N$  time steps and each time step has noise channels acting on a particular site. In the current scenario we set  $n_c=4$ .

the initial entanglement. Note the important point that  $\mathbb{1}/D = \otimes_{j=1}^N \mathbb{1}_j/2$  is generated by, and factorizes into, local identity operators.

To quantitatively understand this phenomena we compute a purity-based fidelity,  $\mathcal{F}_P(\rho, \sigma)$ . With  $|\Psi\rangle, |\Phi\rangle$  as purifications of states  $\rho$  and  $\sigma$  respectively, the Uhlmann-Josza fidelity quantifies the closeness of states as

$$\mathcal{F}_{UJ}(\rho, \sigma) := \max_{\{|\Psi\rangle, |\Phi\rangle\}} |\langle \Psi | \Phi \rangle|^2 = \text{Tr}[\sqrt{\sqrt{\rho}\sigma\sqrt{\rho}}]^2. \quad (11)$$

Due to the difficulty of computing  $\mathcal{F}_{UJ}$ , the Hilbert-Schmidt inner product (HSIP),  $\text{Tr}[\rho\sigma]$  has recently been investigated in terms of computing alternative fidelities which satisfy Josza's axioms [11]. Rather than its self-fidelity, HSIP yields the *purity* of a state,  $P(\rho) := \text{Tr}[\rho^2] \leq 1$ , with the equality holding only for pure states. However, the purity turns out to be a useful normalization function leading to the following alternative fidelity metric [11] given by

$$\mathcal{F}_P(\rho, \sigma) = \frac{\text{Tr}[\rho\sigma]}{\max(P(\rho), P(\sigma))}. \quad (12)$$

The legend in Fig. 2 indicates the fidelity is being taken with respect to random MPS with entanglement quantified by the bond dimension  $\chi$ . The initially distinct states, as a function of time, flow towards one another with the fidelities likewise flowing to unity. This illus-

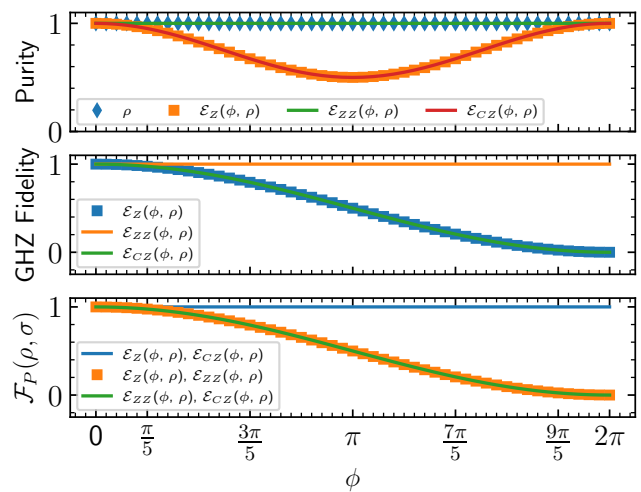


Figure 3. (Top) Purity of ideal GHZ (diamonds) versus that of a GHZ state corrupted by quantum channel described in terms of  $Z_i, Z_i Z_{i+1}$ , or  $C_i Z_{i+1}$  (squares, green, and red lines respectively) Kraus operators. The bare GHZ state and  $Z_i Z_{i+1}$  noised gates remain pure ( $P = 1$ ) while, the  $Z_i$  and  $C_i Z_{i+1}$  noised states have minimal purity  $P = 1/2$  at  $\phi = 2 \arcsin(\sqrt{\alpha}) = \pi$  where  $\phi$  parameterizes dissipative rates of the Kraus operators [13]. (Middle) Fidelity between the ideal GHZ state and damped variants. The action of  $Z_i Z_j$  stabilizes the state, while the  $Z_i$  and  $C_{i-1} Z_i$  gates also act identically and phase damp the GHZ state. (Bottom) Purity based fidelity of noised quantum states. Since  $Z_i$  and  $C_{i-1} Z_i$  dissipators act on the GHZ state identically, the fidelity of these two states is unity, but below unity when computing fidelity with respect to other states. We note that the results are computed for a system size of  $N = 500$ , however these hold even in the thermodynamic limit of  $N \rightarrow \infty$ .

trates how, after a short mixing time, the completely depolarized state is the fixed-point attractor of the local Kraus dynamics. To perform the simulations, we program the `MPrho` type from the base types defined in the `ITensors.jl` [12] julia library. All the simulations are single core, single thread computations run on Intel Core Ultra 7 processor.

## B. GHZ stability under two-local channels

While methods for the application of single-body noise channels have been largely explored, methods for the two-local counterpart are more complicated. Namely, prior algorithms returning the states to the canonical form rely on optimization methods [8]. This optimization hinders the scalability of simulation protocols involving two-local channels. To this end, we introduce an optimization free protocol that allows for the application of two-local noisy channels (see App. C for the details of the protocol). In short, the mixture correlations are heuristically assigned to the  $\kappa$  index of one of the two sites involved in the two-body channel.

To numerically validate our method, we apply distinct two-body noise channels on a  $N$ -qubit GHZ state:  $|\phi\rangle = \frac{1}{\sqrt{2}}(|0\rangle^{\otimes N} + |1\rangle^{\otimes N})$ . Using  $|\mathbf{0}\rangle = |0\rangle^{\otimes N}$ , the initial density matrix is given by  $\rho_{GHZ} = 1/2(|\mathbf{0}\rangle\langle\mathbf{0}| + |\mathbf{0}\rangle\langle\mathbf{1}| + |\mathbf{1}\rangle\langle\mathbf{0}| + |\mathbf{1}\rangle\langle\mathbf{1}|)$ . The analytic properties of the GHZ state provide a good testing platform to verify our results.

Consider the action of quantum channels with three different types of dephasing noise. In the operator sum representation, these channels are described in terms of the Kraus operators:  $K_0^{ZZ} = \mathbb{1}$  and  $K_1^{ZZ} = Z_i Z_{i+1}$ ,  $K_0^Z = \mathbb{1}$  and  $K_1^Z = Z_i$ , and  $K_0^{CZ} = \mathbb{1}$  and  $K_1^{CZ} = CZ_{i,j}$ . Here  $Z_i$  is the phase-flip as defined earlier,  $CZ_{i,j}$  represents the controlled- $Z$  gate with  $i(j)$  as the control(target) qubit. Note that, instead of decohering, the GHZ state is stabilized as an  $+1$  eigenstate of both  $K_0^{ZZ}$  and  $K_1^{ZZ}$ . Under the action of under  $CZ$  the zero branch is not dephased while the one term is dephased, identically as under the action of  $Z$ . In Fig. 3 we compute the purity, fidelity with original GHZ state, and mutual fidelity  $\mathcal{F}_P(\rho, \sigma)$  under the action of the above noisy channels and note the agreement with the analytic results.

### C. Erasure as a source of global mixtures

In this section, we analyze trace as an operation to generate *global* mixture correlations. This is a limit which, to the best of our knowledge and despite its importance to experiments, has not been carefully examined within the LPDO formalism. By tracing out a sub-system, we will highlight both the ability to re-gauge global mixture correlations as well as recover the analytic isometric properties which are important defining features of the MPS and  $MP\rho$ . Note that, while mixture correlations may be decomposed and structured according to their locality properties, the movement of all correlations in a global manner is a limit worth examining due to the ubiquitous nature of global mixture correlations.

One of the simplest and paradigmatic physical examples where trace manifests is in single particle erasure<sup>3</sup>. We model erasure of the  $i^{\text{th}}$  qubit by a partial trace over the  $i^{\text{th}}$  subsystem, leaving its  $\bar{i}^{\text{th}}$  complement behind. The operation as map on density matrix is given by  $\rho \rightarrow \rho_{\bar{i}} = \text{Tr}_i[\rho]$ . The corresponding erasure channel in the  $MP\rho$  formalism is to trace out the tensor. Explicitly, as illustrated in Fig. 4, this involves tracing over the physical degree of freedom,  $s_i$  and the corresponding decorated mixture index,  $\kappa_i$ . Further, the corresponding latent virtual indices are contracted with an adjacent site, either  $i-1$  or  $i$ . Tab. 1 outlines the algorithm for an erasure channel in the context of general quantum dynamics.

<sup>3</sup> e.g. imagine an atomic trap where one atom is ejected from the trap. In this case one may not even know *which* atom was lost, nullifying the notion of a third, flagged erasure state

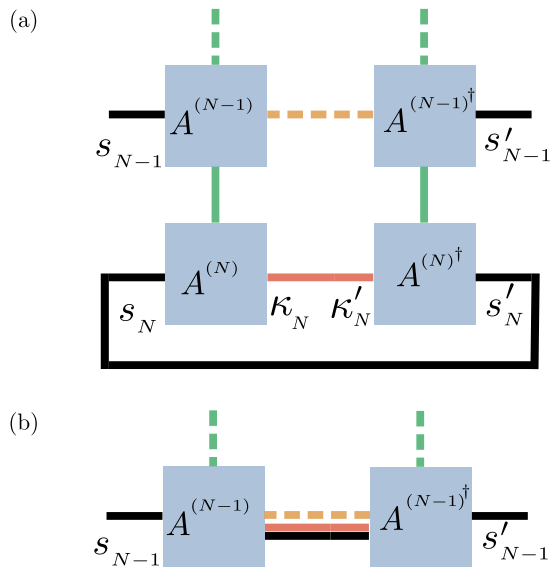


Figure 4. Tracing over local spin degrees of freedom contribute to the mixture correlations. Tracing out site  $s_N$ , involves (a) tracing over the physical indices, the corresponding  $\kappa_N$  indices and contracting over the virtual indices (the  $\chi$ -index), (b) local spin degrees are merged into the mixture index,  $\kappa_{N-1}$  on the neighboring site.

---

#### Algorithm 1 Erasure channel correlation conversion

---

- 1: Select the  $i^{\text{th}}$  qubit to erase. Reshape the tensor so that its physical indices and mixture indices are reshaped into a common index,
  - 2: Contract the virtual indices (connecting with the  $(i-1)^{\text{th}}$  or  $(i+1)^{\text{th}}$  tensors),
  - 3: Re-orthogonalize the  $MP\rho$ , keeping the mixture indices with the orthogonality center, as desired,
  - 4: Continue to apply one- and two-body unitaries or noise channels as the simulation requires.
- 

#### Gauging global correlations

In the following, we analyze the partial trace in the context of the GHZ state. The partial trace operation a qubit  $i$  can be viewed as a map in the operator sum representation with Kraus operators given by  $K_0 = \langle 0|_i$  and  $K_1 = \langle 1|_i$ . Partial trace of any spin results in the state  $\mathcal{E}_E(\rho_{GHZ}) = 1/2(|\mathbf{0}\rangle\langle\mathbf{0}| + |\mathbf{1}\rangle\langle\mathbf{1}|)$ , where the  $|\mathbf{0}\rangle$  now represents tensor product over the remaining  $N-1$  sites. As a result of partial trace, the off diagonal coherence correlations have been converted into diagonal mixture correlations. That is, we now have  $p_0 = p_1 = \frac{1}{2}$  and both of these mixture components contain only one coherence correlation ( $c_{0,\dots,0} = 1$  or  $c_{1,\dots,1} = 1$  respectively) which has been renormalized to unity.

The partial trace above highlights a few important but distinct invariances. The first being that we could have traced *any* qubit with the result still holding the same global correlations. This is a consequence of the permu-

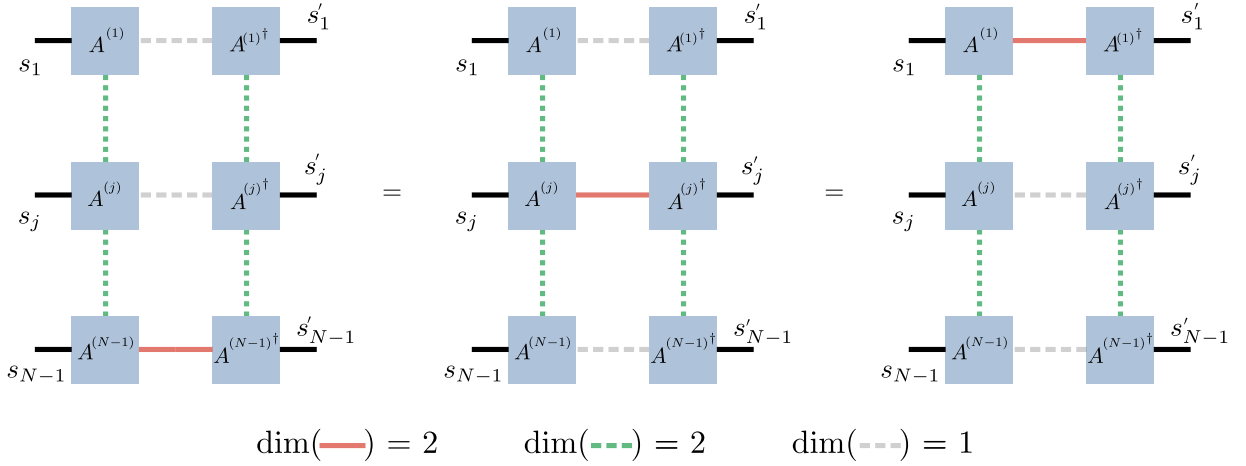


Figure 5. In the context of the GHZ state, after tracing out the  $N^{\text{th}}$  qubit, the  $\text{MP}\rho$  is internally re-gauged. This results in the freedom to store/transfer the mixture correlations at any site (left)  $N - 1$ , (middle) some intermediate site  $j$ , (right) first site as indicated by the 2-dimensional  $\kappa$  index at the respective sites highlighted with a thick orange bond.

tation invariance of the GHZ state. Secondly, we may, after trace, translate the location of the dimension-2  $\kappa$ -index to any site of choice as highlighted in Fig. 5.

Consequently, we see how  $\text{MP}\rho$ 's latent invariances, in the possible representations one can gauge, enable some freedom in representing the mixture correlations. In this example, mixture correlations can be translated in the vertical direction as in Fig. 5. This is achieved by contracting nearest neighbor tensors and then setting the dimensions of the desired SVD as per the two-body optimization free update (App. C). Explicitly, in the case of a traced out qubit of the GHZ state, one sets the kappa index from 2 to 1, on the tensor currently with the index, while setting the kappa index from 1 to 2, on the tensor which will encode the mixture correlations after the next update.

#### Unitary freedom and Non-Uniqueness

Earlier, in Sec. III A, we described  $\rho$ , a mixed state, as a sum of positive operators  $\vec{A}_k \vec{A}_k^\dagger$  weighed by the corresponding mixture probability coefficients,  $\vec{p}_k$ . In the following, we highlight the invariance of  $\rho$  under the action of an internal transformation. That is, the action of isometries on  $\vec{A}_k$ 's  $\kappa$ -subspace, as illustrated in Fig. 6 (b) leaves the mixed state invariant. As a result, the mixture sum representation is non-unique and  $\rho$  is represented up to an equivalence class of (most generally isometric) transformations of the  $\kappa$ -subspace. That is,

$$\begin{aligned} \rho &= \sum_k p_k A_k A_k^\dagger \\ &= \sum_k p_k A_k U U^\dagger A_k^\dagger \end{aligned} \quad (13)$$

$$= \sum_{k'} p_{k'} \tilde{A}_{k'} \tilde{A}_{k'}^\dagger = \rho'$$

As an explicit example, consider the computational basis states,  $|0\rangle_N, |1\rangle_N$ , of the traced out qubit. Each of them was initially coherently correlated with the rest of the spin-chain. Note that all entanglement properties of the system are invariant under local  $SU(2)$  transformations. Additionally note that observable quantities are defined with respect to the basis independent trace  $\langle \hat{A} \rangle = \text{Tr}[\hat{A}\rho]$ . Fig. 6 (b) illustrates the freedom to unitarily transform a tensor across the local virtual mixture index. In the present case, of tracing a single qubit from a multi-qubit GHZ, the unitary freedom acts as an  $SU(2)$  on the two Feynmann paths, which are the (now rotated) computational basis states that were traced over in Fig. 4. The invariance between  $\rho$  and  $\rho'$  is proved by recalling that all observables are independent of the choice of basis when tracing out the qubit.

## V. CONCLUSION

In this work we have examined the operational interpretation of  $\text{MP}\rho$  as a classical-quantum data structure that encodes both complex coherence and real mixture correlations. Building on prior LPDO efforts, our work develops technical algorithms to update the canonical form while also developing a physical and operational interpretation for the degrees of freedom encoded by the virtual mixture indices. In short, this investigation expands the computational tool-set for working with density operators at scale.

Within the  $\text{MP}\rho$  formalism we have first examined the evolution of entangled quantum states under the action of one- and two-local quantum channels. Previously, the action of two-local channel operators was defined in terms of a SVD in conjunction with a bond-dimension-

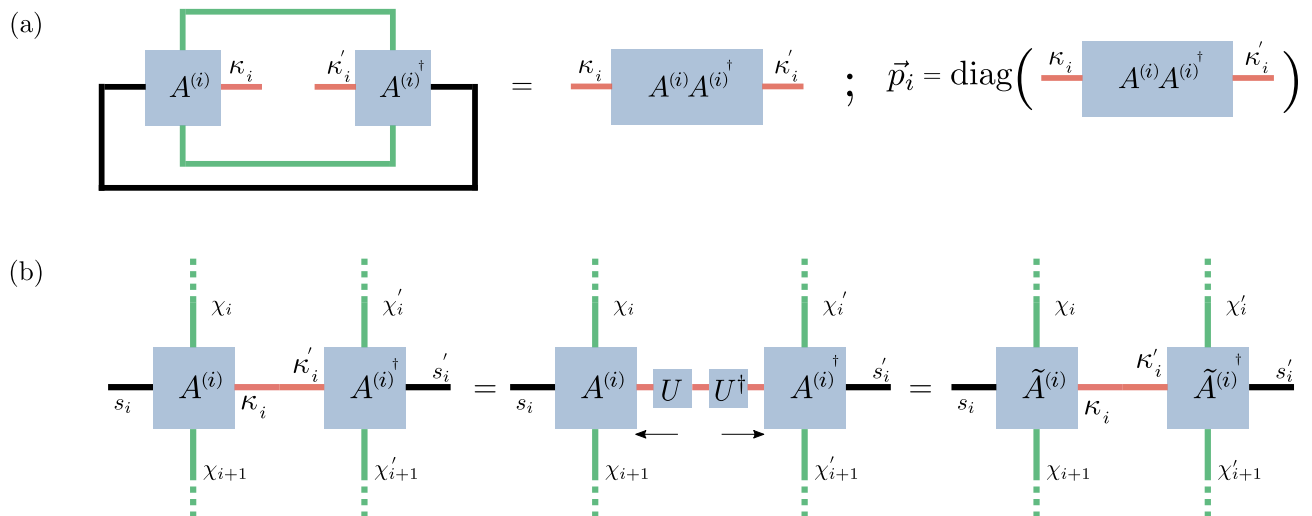


Figure 6. Isometric gauge freedom of  $\text{MP}\rho$ . (a) Procedure to obtain the probabilities,  $\vec{p}_i$  corresponding to the  $\kappa$ -subspaces at site,  $s_i$ . (b) Isometric action in the subspaces leaves the corresponding  $\rho$  invariant, thereby highlighting its non-unique representation using  $\text{MP}\rho$ . This is similar to the non-unique representation of MPS as discussed in Fig. 7.

minimizing optimization routine [8]. To simplify the application of two-local noise channels, we develop an optimization-free update which returns the tensors, contracted under the application of a two-body channel, back to the canonical form. To verify our technique, we have tested the application of two-body noise channels within the context of an analytically solvable example. Lastly, we present an algorithm that elucidates partial trace in the  $\text{MP}\rho$  formalism and highlight the representation of global mixture correlations within a local gauge.

To stress test the computational capabilities of this framework, we present several numerical simulations involving single and two-body channel operators. For example, we have dissipatively evolved initial random  $\chi$ -entangled 50-qubit density operators. In contrast, naive simulations of density operators within a state-vector format are limited to systems with fewer than 25 qubits, even at supercomputing scales. Our work, therefore, highlights the large locus of mixed quantum states which are amenable to a classical multi-linear representation and subsequently simulation.

The  $\text{MP}\rho$  formalism provides tools to explore avenues that have been recently gaining traction [14, 15]. For example, analyzing the dynamics of many-body systems in an open setting i.e., in the presence of the noise, can be hugely accelerated [16–18]. The simulation of quantum systems necessitating supercomputer resources, thereby strongly demarcating the classical simulable limits, remains an intriguing open question [19]. We conjecture that, in future work, sampling of the decorated mixture index will be useful in parallelized algorithms which themselves might provide crucial insights into the fundamental limits of simulating open quantum systems.

From an experimental viewpoint,  $\text{MP}\rho$  tools can be deployed to not only characterize, but also subsequently mitigate, errors in current quantum architec-

tures, thereby proving a useful tool for future quantum control theory [20]. A last future grand challenge is to analyze quantum algorithms, in terms of their computational complexity, in the presence of realistic noise models and, if possible, to optimize the associated performance metrics.

During the writing of this manuscript Refs. 9, 14 appeared. These works also target simulations of noisy quantum systems, in terms of positive matrix product operators, but differ from our algorithm and results.

## VI. ACKNOWLEDGEMENTS

E.D. and A.J. are supported by the U.S. Department of Energy, Office of Science, Advanced Scientific Research Program, Early Career Award under contract number ERKJ420. We thank A. Nocera, G. Alvarez, B. Xiao, V. Protopopescu, and ORNL’s Quantum Information Science Section for valuable discussions.

### Appendix A: The coherence correlation tensor

In this appendix, we briefly present the different approaches involved in representing the coherent correlations,  $\mathbf{c}$ . One is a global perspective, wherein  $\mathbf{c}$  is vectorized into a 1-tensor by grouping all the indices together into a global  $2^N$ -dimensional index such that  $\mathbf{c} := \mathbb{C}^{2^N} \rightarrow \mathbb{C}$ . In other words, for given a computational basis vector, a complex amplitude associated to the bit string is returned, as  $\mathbf{c} := \mathbb{C}^2 \otimes \mathbb{C}^2 \otimes \dots \otimes \mathbb{C}^2 \rightarrow \mathbb{C}$ . Given this *local* tensor product structure  $\mathbf{c}$  is an  $N$ -linear tensor, where each index is two-dimensional.

MLReps of  $\mathbf{c}$  go beyond this by encoding the complex



correlations as a function of additional virtual indices. This is somewhat counter-intuitive as virtual indices are not a necessary condition and seemingly add complexity. However, as discussed in the main text, they provide a systematic way to express locus of states with only polynomial numbers of non-zero correlations in a scalable manner. Explicitly Eq. 2 uses

$$\mathbf{c} = \text{Tr}_\chi[A^{(1)} \dots A^{(N)}]. \quad (\text{A1})$$

By inserting and re-contracting invertible matrices  $R_i$  and  $R_i^{-1}$  at the  $i^{\text{th}}$  bond, Fig. 7 graphically proves the non-uniqueness of an infinite 1D tensor train. By judiciously leveraging this freedom, we can write the MPS in a left/right/mixed canonical form, using and enforcing Eq. 4a and Eq. 4b, for further details see Ref. 5.

### Appendix B: U(1) gauge-invariance

As a gauge invariance warm up, consider a global  $U(1)$  transformation  $|\psi_k\rangle \rightarrow e^{i\phi}|\psi_k\rangle$ . This transforms the statistical ensemble as:  $\rho \rightarrow \sum_k p_k e^{i\phi} |\psi_k\rangle \langle \psi_k| e^{-i\phi} = \rho$ . Since each of the  $p_k$ 's is positive we may write them in the complex polar form as  $p_k = |p_k| e^{\text{Arg}(p_k)} = |p_k|$ . This latent gauge transformation ensures that the mixture coefficients remain positive, non-complex quantities. That is, we can absorb these phases into the mixture *eigenvalues* with opposing phases  $\sqrt{p_k} e^{i\phi} \times \sqrt{p_k} e^{-i\phi} = p_k$ . This phase cancellation thus provide an intuition for how other latent, locally invariant, gauged degrees of freedom work leading to the construction of equivalent  $|\Psi\rangle$ - and  $\rho$ -representations.

### Appendix C: Gauge fixing two-body channels

In this appendix, we present the operational procedure employed in applying a two-body channel operator. A key highlight of our approach, as elucidated in the main text, is that the method introduced is optimization free, in comparison to other approaches wherein they rely on optimization routines in realizing the same [8]. We outline the steps involved in realizing the operation in Fig. 8 and note the multiplicative gauge freedom in  $\kappa_{i,i+1} = \kappa_i \otimes \mathbb{1}_{i+1} = \mathbb{1}_i \otimes \kappa_{i+1}$ , e.g. if  $\dim(\kappa_i) = \dim(\kappa_{i,i+1})$ , is fixed thereby allowing the procedure to

scale. One other interesting fact is that we retain the  $\text{MP}\rho$  canonical form post the application of the channel.

### Appendix D: The operator sum representation

Let us examine some properties of quantum channels and their impact on mixture and coherence correlations. In the operator sum representation we have a quantum channel expanded as a sum over a basis of  $L$  Krauss operators,

$$\mathcal{E}(\rho) = \sum_{k=1}^{k=L} F_k \rho F_k^\dagger. \quad (\text{D1})$$

In order to derive a symmetry operator, separating the coherence correlations and the mixture correlations so that we can represent them with additive scaling, let us examine the action of unitaries and quantum channels on *coherence* (not mixture) correlations.

First, it is well known that the norm of the state's coherence correlations is unitarily invariant. That is, if  $|\Phi\rangle = U|\Psi\rangle$  then  $\sum_i |c_i^{(\Phi)}|^2 = \sum_i |c_i^{(\Psi)}|^2 = 1$ . In either case, the norm of the coherences is manifestly preserved and the *mixture* correlations are also invariant under such an operation since,

$$\begin{aligned} U\rho U^\dagger &= \sum_{k=1}^{\kappa} p_k U|\psi_k\rangle \langle \psi_k| U^\dagger \\ &= \sum_{k=1}^{\kappa} p_k |\phi_k\rangle \langle \phi_k|. \end{aligned} \quad (\text{D2})$$

Again, the mixture correlations are  $\vec{p}$  in both cases, with only difference being that the coherence correlations have been reshuffled but their Euclidean norm preserved. In this special case, of a unitary quantum channel with  $L = 1$ , the number of mixture correlations is *non-increasing*.

On the other hand, a quantum channel described by  $k > 1$  Kraus operators may modify both the coherence and the mixture correlations. As a general rule, a quantum channel with  $L$  Kraus operators (in its minimal description) decreases the number of coherence correlations if it consists of one-body operators. Depending on the form of both the input state and the quantum channel the number of mixture correlations may increase from  $\kappa$  to a maximum of  $L\kappa$  or the number of mixture correlations may decrease to the minimum of 1.

---

[1] S. R. White, Density matrix formulation for quantum renormalization groups, *Physical Review Letters* **69**, 2863 (1992).  
 [2] M. P. Zaletel and F. Pollmann, Isometric Tensor Network States in Two Dimensions, *Physical Review Letters* **124**, 037201 (2020), [arXiv:1902.05100](https://arxiv.org/abs/1902.05100).

[3] D. Perez-Garcia, F. Verstraete, M. M. Wolf, and J. I. Cirac, Matrix product state representations, *Quantum Information and Computation* **7**, 401 (2007), [arXiv:0608197](https://arxiv.org/abs/0608197) [quant-ph].  
 [4] F. Verstraete, V. Murg, and J. Cirac, Matrix product states, projected entangled pair states, and variational

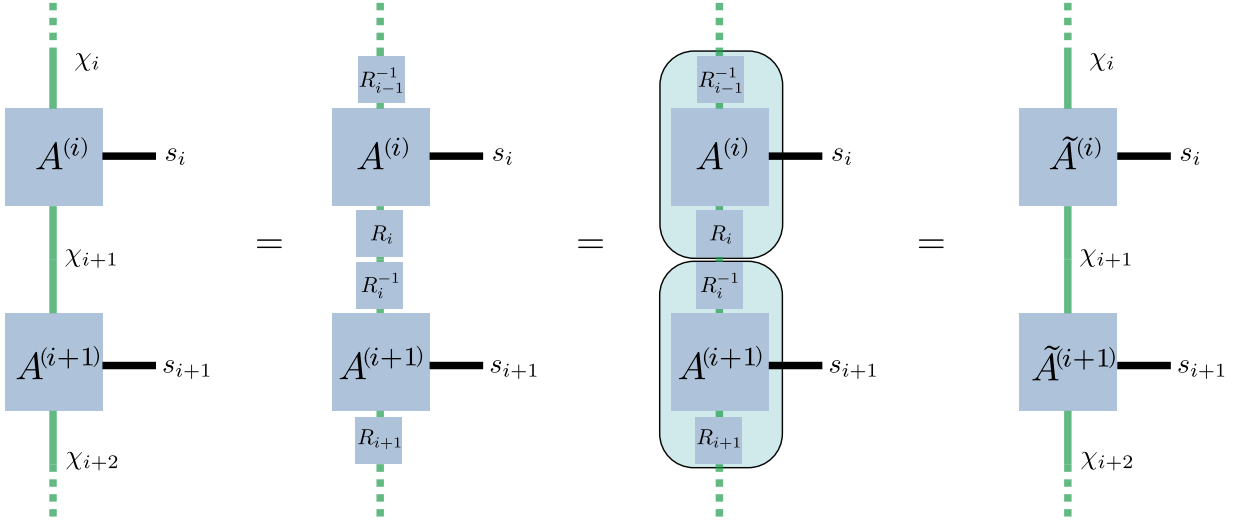


Figure 7. Non-uniqueness of MPS-representation as a mathematical gauge invariance. Injecting  $\chi_i$ -dimensional matrix resolutions of identity  $R_i R_i^{-1} = \mathbb{1}_{\chi_i}$  into the first column's virtual correlation spaces results in the second column. Contracting the third column's shaded regions results in the fourth column's equivalent representation.

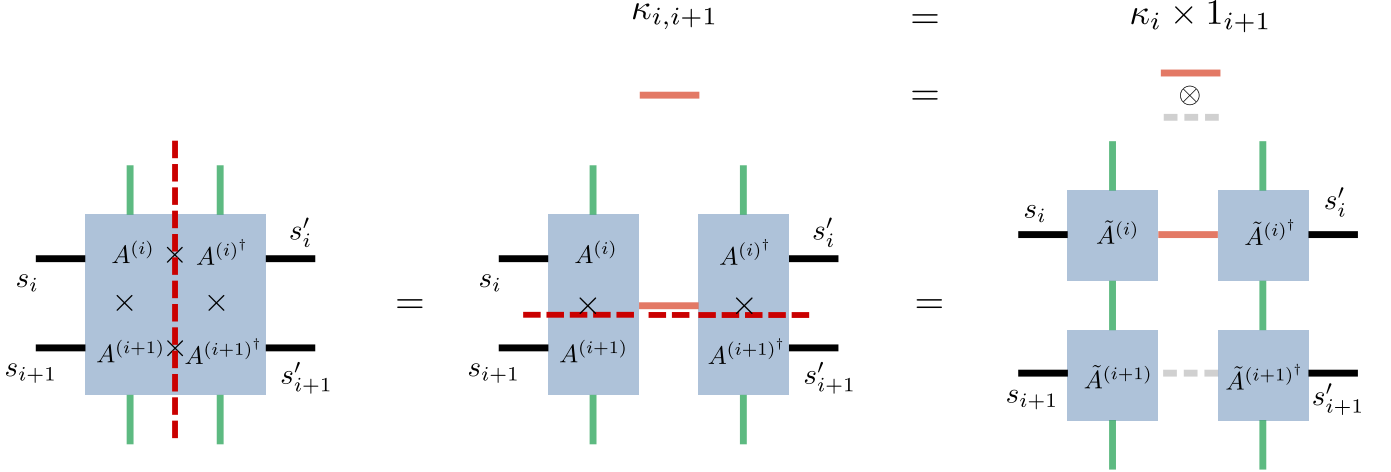


Figure 8. Optimization free routine for the application of the two-body noise channel. (Left) Factorization of  $\rho_{i,i+1} = \sum_{k=1}^{\kappa_{i,i+1}} A^{(i,i+1)}[:,k] A^{(i,i+1)\dagger}[:,k]^\dagger$ . (Middle, Right) SVD performed across the site-wise bi-partition, by expressing  $\kappa_{i,i+1} = \kappa_i \otimes \mathbb{1}_{i+1}$ , where  $\kappa_i = \kappa_{i,i+1}$ . The above decomposition results in a valid MP $\rho$  canonical form. The red dashed line represents decomposition using SVD.

renormalization group methods for quantum spin systems, *Advances in Physics* **57**, 143–224 (2008).

- [5] U. Schollwöck, The density-matrix renormalization group in the age of matrix product states, *Annals of Physics* **326**, 96 (2011), january 2011 Special Issue.
- [6] G. D. I. Cuevas, N. Schuch, D. Pérez-García, and J. Ignacio Cirac, Purifications of multipartite states: limitations and constructive methods, *New Journal of Physics* **15**, 123021 (2013).
- [7] F. Verstraete, J. J. García-Ripoll, and J. I. Cirac, Matrix product density operators: Simulation of finite-temperature and dissipative systems, *Physical Review Letters* **93**, 10.1103/physrevlett.93.207204 (2004).
- [8] A. H. Werner, D. Jaschke, P. Silvi, M. Kliesch,

T. Calarco, J. Eisert, and S. Montangero, Positive tensor network approach for simulating open quantum many-body systems, *Phys. Rev. Lett.* **116**, 237201 (2016).

- [9] M. Ambrose, A. Thomas, and B. Coeurtin, Enabling large-depth simulation of noisy quantum circuits with positive tensor networks, (2024).
- [10] S. Cheng, C. Cao, C. Zhang, Y. Liu, S.-Y. Hou, P. Xu, and B. Zeng, Simulating noisy quantum circuits with matrix product density operators, *Physical Review Research* **3**, 10.1103/physrevresearch.3.023005 (2021).
- [11] Y.-C. Liang, Y.-H. Yeh, P. E. M. F. Mendonça, R. Y. Teh, M. D. Reid, and P. D. Drummond, Quantum fidelity measures for mixed states, *Reports on Progress in Physics* **82**, 076001 (2019).

- [12] M. Fishman, S. R. White, and E. M. Stoudenmire, The ITensor Software Library for Tensor Network Calculations, *SciPost Phys. Codebases*, 4 (2022).
- [13] M. A. Nielsen and I. L. Chuang, *Quantum Computation and Quantum Information: 10th Anniversary Edition* (Cambridge University Press, 2011).
- [14] K. Kato, [Exact renormalization group flow for matrix product density operators](#) (2024), [arXiv:2410.22696 \[quant-ph\]](#).
- [15] S. Srinivasan, S. Adhikary, J. Miller, B. Pokharel, G. Rabusseau, and B. Boots, Towards a trace-preserving tensor network representation of quantum channels (2021).
- [16] J. Shah, C. Fechisin, Y.-X. Wang, J. T. Iosue, J. D. Watson, Y.-Q. Wang, B. Ware, A. V. Gorshkov, and C.-J. Lin, [Instability of steady-state mixed-state symmetry-protected topological order to strong-to-weak spontaneous symmetry breaking](#) (2024), [arXiv:2410.12900 \[quant-ph\]](#).
- [17] S. Sun, J.-H. Zhang, Z. Bi, and Y. You, [Holographic view of mixed-state symmetry-protected topological phases in open quantum systems](#) (2024), [arXiv:2410.08205 \[quant-ph\]](#).
- [18] Y.-H. Chen and T. Grover, Separability transitions in topological states induced by local decoherence, *Phys. Rev. Lett.* **132**, 170602 (2024).
- [19] Z. Chen, Y. Bao, and S. Choi, [Optimized trajectory unraveling for classical simulation of noisy quantum dynamics](#) (2023), [arXiv:2306.17161 \[quant-ph\]](#).
- [20] S. Mangini, M. Cattaneo, D. Cavalcanti, S. Filippov, M. A. C. Rossi, and G. García-Pérez, Tensor network noise characterization for near-term quantum computers, *Physical Review Research* **6**, 10.1103/physrevresearch.6.033217 (2024).